COMMUNICATION

Rollable Transparent Glass-Fabric Reinforced Composite Substrate for Flexible Devices

By *JungHo Jin, Ji-Hoon Ko, SeungCheol Yang,* and *Byeong-Soo Bae**

Recently, there has been considerable interest in flexible displays, as they facilitate the fabrication of displays that are thin, lightweight, robust, conformable, and flexible.[1] To enable a flexible display, a flexible substrate must be used as the fundamental starting component in place of a conventional glass substrate. In general, metal foils, ultra-thin glasses, and plastic films are considered candidates for a flexible substrate.[2] In particular, flexible displays using plastic substrates based on organic polymers have been a major topic not only because these show outstanding flexibility and optical clarity at the same time, but also because they offer the possibility of a reduction in cost, coupled with a roll-to-roll process and ink-jet printing technology.[3] Common examples of commercially available polymers are polyethylene terephthalate (PET), polyether sulfone (PES), polyethylene naphthalate (PEN), polycarbonate (PC), and polyimide (PI).[1,4] To replace conventionally used glass substrates, a plastic substrate must be equipped with the properties of glass, such as optical transparency, thermal/chemical stability, O_2/H_2O permeability, low birefringence (or retardation), dimensional stability, and a low coefficient of thermal expansion (CTE).[1] Among these properties, the low CTE of plastic substrates coupled with dimensional stability is arguably the most important requirement, as it is directly related to compatibility with all other necessary display layers to be integrated onto them.[1] Although there have been extensive studies of flexible devices built on polymer substrates, such as electrophoretic displays and organic thin-film transistors (OTFTs), little progress have been made even with high-temperature processed devices such as active-matrix liquid crystal displays (AMLCDs).[5] Major obstacles include the high CTEs of polymers insufficient for the display layer integrations. Moreover, polymers usually have low glass transition temperatures (T_gs) where abrupt CTE changes are accompanied. This greatly limits their practical application in terms of the process temperature. Even polymers with a high T_g, e.g., PES, are known to have a CTE of ~50 ppm K^{-1}, much higher than the typically required level (less than 20 ppm K^{-1}).[1] Other high-T_g polymers such as polytetrafluoroethylene (PTFE) and poly(ether ether ketone) (PEEK) also have significant drawbacks for implementation into large-area plastic electronics, as they are unfavorable in terms of cost. PI has a low CTE of ~20 ppm K^{-1} and a high T_g, but its practical use is nonetheless problematic because of the high birefringence and yellowness.

In the present study, we report a novel high-performance transparent glass-fabric reinforced composite film (GFRHybrimer) which can be used as a substrate for flexible devices. The GFRHybrimer film was fabricated by impregnation and/or lamination of a woven glass-fabric (or glass cloth) with a photocurable, oligosiloxane-based hybrid material (hybrimer) as the matrix.[6] In terms of material, the use of such an organic/inorganic hybrid-type matrix offers versatile properties such as chemical inertness, thermal stability, optical transparency, and ease of functionalization. These properties originate from the desirable nature of organic/inorganic phases which are synergistically combined to form a homogeneous hybrid network. In addition, the glass-fabric reinforcement enables not only a significant reduction in the CTE, but also a remarkable increase in the modulus and flexibility. We used a 25 μm thick E-glass cloth (**Figure 1b**) whose CTE is of ~5.5 ppm K^{-1}. First, the glass-fabric was fired under an ambient atmosphere at 500 °C for 30 min to burn out the organic sizing agent coated onto its surface. Two sheets of the glass-fabric were then stacked and placed on a glass plate (Figure 1a). Two sheets of glass-fabric were used for easy handling because a composite film fabricated with one sheet was too thin for further processing. The glass-fabrics were then impregnated with the matrix resin which is a clear, viscous, UV-curable resin (**Figure 2a**). The drenched sample was then covered with another glass plate (Figure 1a). To obtain a proper film thickness, a vacuum bag press molding technique was used to press the sandwiched sample uniformly, which is a typical fabrication method for sheet molding compounds (SMCs). With this method, we could not only control the film thickness to be optimized by controlling the vacuum pressure, but also effectively eliminate air pores entrapped inside the film. The sample was then UV-cured and heat-treated at 180 °C for 4 h to obtain a flexible, transparent composite film (Figure 1e). The optimized film thickness was approximately 55–60 μm (Figure 1c). A film thickness less than 50 μm was unfavorable because the glass-fabrics could be exposed to the film surface, which can cause haziness and non-uniformity of the film. According to our scanning electron microscopy (SEM) analysis, the surface of the GFRHybrimer film was flat and smooth (Figure 1d). The root mean square (RMS) roughness determined from the atomic force microscopy (AFM) analysis was ~1.9 nm (see Figure S1 in the Supporting Information). The GFRHybrimer substrate film was highly flexible to the point that it could even be rolled onto a 3.2 mm mandrel bar without any damage (Figure 1f). Flexibility and mechanical durability of the GFRHybrimer film was tested in a bending test. The GFRHybrimer film tolerated 10^4-times repeated bending cycles

[*] J. Jin, J.-H. Ko, S. Yang, Prof. B.-S. Bae
Laboratory of Optical Materials & Coating
Dept. Materials Science and Engineering
KAIST, 373–1 Guseong-dong, Yuseong-gu,
Daejeon 305–701 (Korea)
E-mail: bsbae@kaist.ac.kr

DOI: 10.1002/adma.201002198

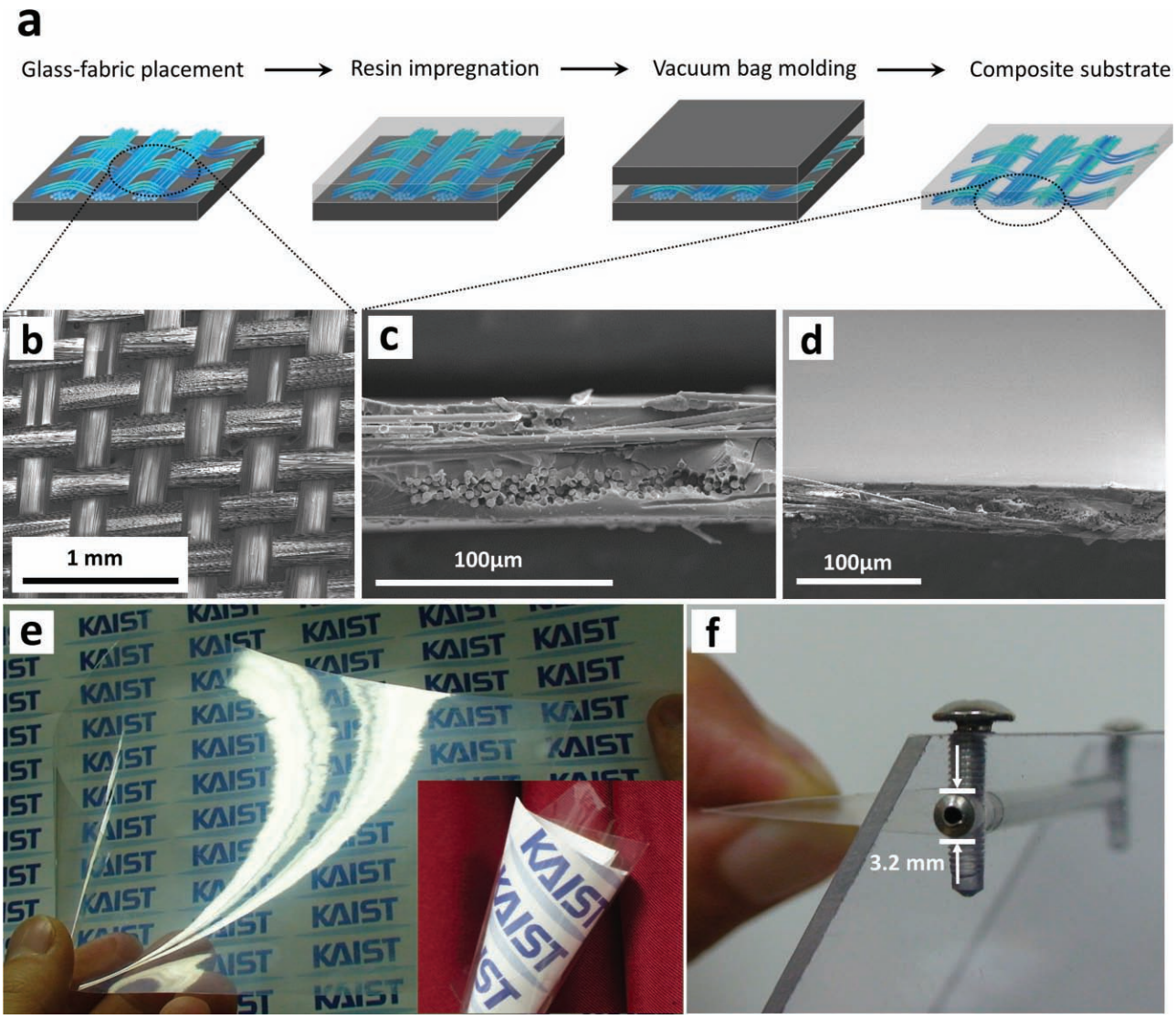

Figure 1. a) Schematic illustration of the fabrication process used for the creation of the GFRHybrimer film. Two sheets of woven glass-fabric were placed on a glass plate. After matrix resin impregnation followed by vacuum bag press molding, the GFRHybrimer film was separated from the two glass plates. In the vacuum bag press molding step, the sample was placed between a silicone bag and a metal plate and was then sealed. When the vacuum was applied, the entrapped air and excess resin in the sample were removed, providing a proper film thickness. b) SEM image of the woven glass-fabric used (E-glass, 25 μm thick). c) and d) SEM images of the GFRHybrimer film (cross-sectional and surface view, respectively). e) Images of the GFRHybrimer film. The inset image shows a rolled-up GFRHybrimer film. f) Image of the GFRHybrimer film rolled up in a 3.2 mm diameter mandrel without any cracking (the mandrel bend test was conducted based on ASTM D522-93a).

without any cracking or surface degradation (see Figure S1 in the Supporting Information)

High optical transparency of the GFRHybrimer film could be obtained by the matching refractive index (n) of the glass-fabric and the matrix. For several beneficial reasons, we used the hybrimer as the matrix, which is a typical hybrid thermoset based on the UV-curing of an organo-oligosiloxane resin synthesized by a sol–gel reaction of 3-(methacryloxy)propyltrimethoxysilane (MPTMS) and diphenyldimethoxysilane (DPDMS) (Figure 2a). Other than the high optical transparency (~90%), the low birefringence (~10^{-4}), the high thermal stability (>370 °C), and the glass-compatible nature originating from the existing Si–OH groups (Figure 2a), major advantages of using the hybrimer as the matrix include 1) its high refractive index (n_D of 1.54–1.57) and 2) its precise refractive index tunability which can be fulfilled by controlling the Si/phenyl molar ratio (r) in the sol–gel reaction (Figure 2b).[6] In particular, the high refractive index of the hybrimer enabled the use of an inexpensive, high-n glass-fabric such as E-glass instead of a high-priced, low-n glass-fabric such as T-glass. We emphasize that this is important in terms of cost given that the price of the composite substrate is mostly determined by the glass-fabric used. The virtue of the refractive index tunability of the hybrimer can be demonstrated by the following equations. The optical transmittance (T) of a continuous glass-fabric reinforced composite is given by[7]

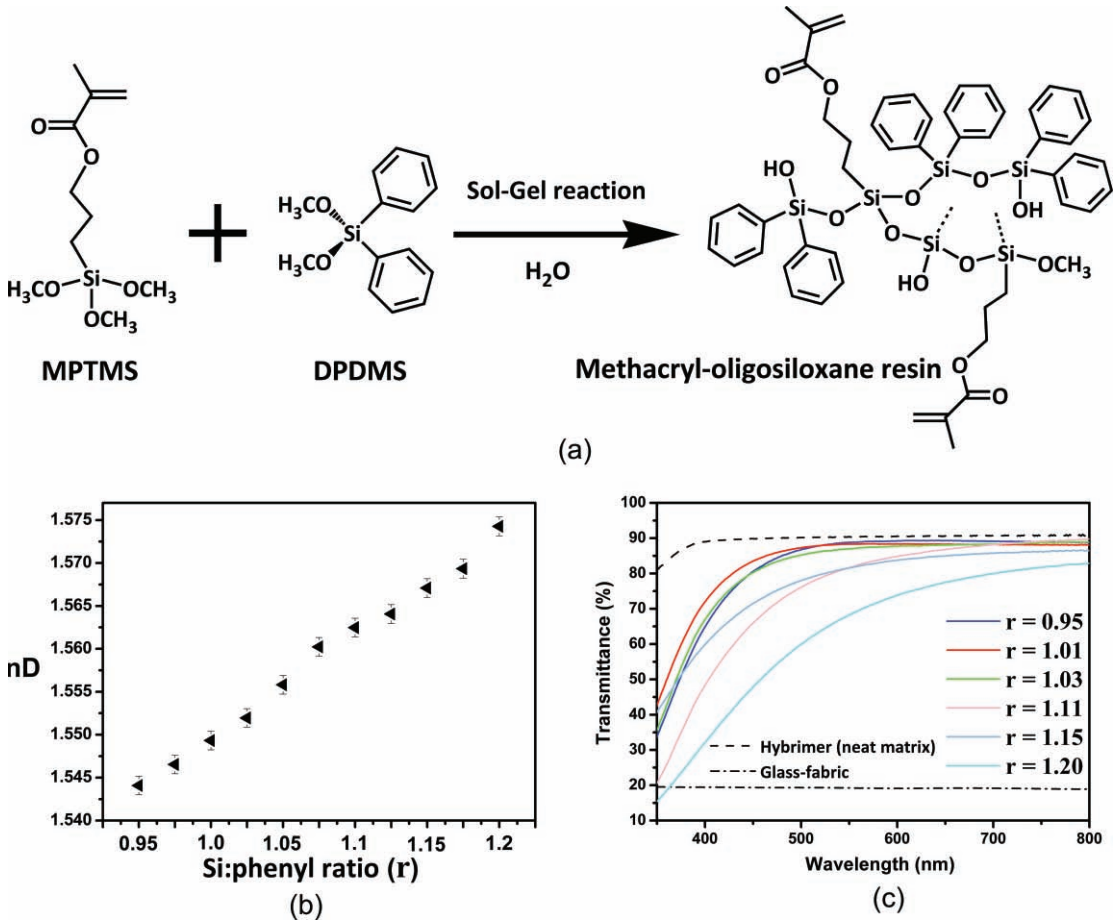

Figure 2. a) Sol–gel reaction scheme of MPTMS and DPDMS to form the methacryl-oligosiloxane resin which is UV-cured (hybrimer matrix). Si/phenyl molar ratio can be controlled with DPDMS amount. b) Plot of n_D vs. the Si/phenyl molar ratio (r) as measured by an Abbe refractometer. c) Optical transmittances of the GFRHybrimer films with various *r* values as measured by a UV-vis spectrophotometer.

$$T = \left[1 - 2Q_{ext}(\rho)\left(\frac{f}{\pi}\right)^{1/2}\right]^{(d/R_f)(f/\pi)^{1/2}} \quad (1)$$

where Q_{ext} is defined as the scattering efficiency factor, ρ is the phase lag of light passing through the fiber, f is the volume fraction of the fiber, d is the total thickness of the composite and R_f is the fiber radius. Q_{ext} is a function of ρ and is given by

$$Q_{ext}(\rho) = 2\rho\int_0^{\pi/2} \sin(\rho\cos\gamma)\sin^2\gamma\, d\gamma \quad (2)$$

where γ is the angle between the incident light direction and the fiber surface. ρ is then given by

$$\rho = 2\frac{2\pi}{\lambda}R_f|n^f - n^m| \quad (3)$$

where n^f and n^m are the refractive index of the fiber and the matrix, respectively. From the above equations, it can be realized that $|n^f - n^m|$ should be minimized to obtain the minimum Q_{ext}, i.e., the maximum T. As the refractive index of E-glass at the D line (589.2 nm), i.e., n_D, is known to be ~1.547 (or 1.560 for boron-free E-glass), precise refractive index tunability of the matrix is essential in securing high optical transparency.

Figure 2b displays the n_D of the hybrimer with different *r* values, as measured by an Abbe refractometer. The n_D of the hybrimer could be sensitively controlled from 1.542 to 1.574 while varying *r*, which completely covers the possible n_D range of E-glass. Figure 2c is the UV-vis spectra of the GFRHybrimer films, showing the optical transmittances with various *r* values, which clearly shows the $|n^f - n^m|$ dependence of T. Note that the neat hybrimer matrix shows ~90% of transmittance in the visible region, while the transmittance of the glass-fabric remains below 20%. Based on the n_D measurements, GFRHybrimer samples were prepared with a $|n^f - n^m|$ of less than ~0.002 (r = 0.95, 1.01). These showed an optical transmittance of ~89% at 550 nm, which is nearly the same level of transmittance as that of a neat matrix. On the other hand, in samples with $r > 1.11$ ($n_D > 1.562$), the optical transmittances at 550 nm were less than 81% and even less than 69% for $r = 1.20$ ($n_D = 1.572$) due to the severe mismatch of the refractive index (large $|n^f - n^m|$). Despite the considerable degradation in the transmittance, however, some nonetheless exhibited high optical

transmittance levels (~88% for $r = 1.11$) in a longer wavelength region (700–800 nm). This phenomenon can be attributed to the optical dispersion, that is, the variation of the refractive index with wavelength. Generally, the refractive index tends to decrease as the wavelength increases. The degree of dispersion is measured by the Abbe number (ν_D), which is defined as

$$\nu_D = \frac{n_D - 1}{n_F - n_C}$$

where n_F and n_C are the refractive index at the F line (486.1 nm) and C line (656.3 nm), respectively. Thus, a smaller ν_D indicates that the variation in the refractive index of a material with the wavelength is more pronounced. According to our Abbe refractometer measurements, the ν_Ds of samples with $r = 0.95$ and 1.01 ($|n^f - n^m| < \sim 0.002$) were approximately 38, while those with $r = 1.11$ and 1.15 were less than 32 (in general, high-n materials exhibit low ν_Ds). This result indicates that the dispersion curves of the two groups of samples are different. As the maximum optical transmittance is obtained at the intersecting wavelength of the two dispersion curves of the matrix and the glass-fabric, it can be realized that high optical transmittances can be obtained in samples with $r = 1.11$ and 1.15 in the longer wavelength region in spite of the large $|n^f - n^m|$ at the D line. Moreover, from these results, it can be realized that a sufficiently high ν_D of a matrix material is another key requirement for securing high optical transparency in the entire visible wavelength range.

In the following experiments, the thermo-physical properties of the GFRHybrimer film were assessed by thermogravimetric analysis (TGA) and dynamic/thermo-mechanical analysis (DMA/TMA). In the TGA (**Figure 3a**), the 5% weight loss temperature of the GFRHybrimer film was determined to exceed 370 °C. The char yield at 600 °C was over 70%, from which we could expect that the volume fraction of the glass-fabric (f) was approximately 0.7. From the TMA profile (Figure 3b), the effect of the glass-fabric reinforcement can be clearly observed. The CTE of the GFRHybrimer film was determined to be ~13 ppm K^{-1}, while that of the neat hybrimer matrix was >200 ppm K^{-1}. No pronounced glass transition was noted in the TMA profile of the GFRHybrimer. This is in distinct contrast with PEN which exhibited a clear glass transition point at ~130 °C, where the CTE changed drastically from 23 to 81 ppm K^{-1}. However, in the DMA analysis (Figure 3c), we could observe a slight decrease in the storage modulus of the GFRHybrimer through a wide temperature range, which is an indication of a weak, broad glass transition (in general, DMA is a more sensitive tool in detecting a glass transition compared to TMA). This is also in distinct contrast with PEN and PES, in which significant abrupt decreases in the modulus are observed. Compared to these polymer films, the negligibly weak glass transition of the GFRHybrimer film can be attributed to the highly cross-linked organic/inorganic hybrid network structure of the hybrimer matrix. Detailed physical interpretations of this structural effect have been reported in the related literature pertaining to typical siloxane-based hybrid nanocomposite materials.[8]

After all of the characterizations were complete, the performance of the GFRHybrimer film as a flexible substrate was tested

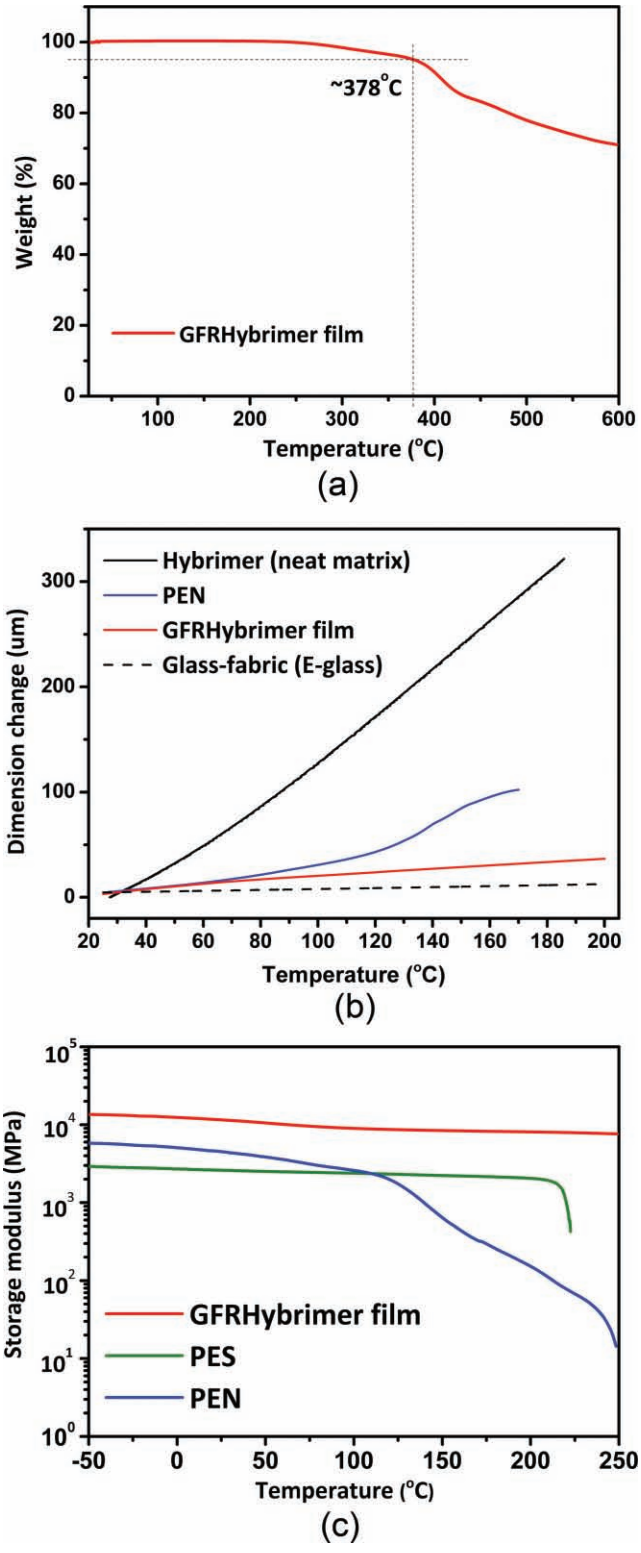

Figure 3. Thermo-physical analyses of the GFRHybrimer film. a) TGA curve (the 5% weight loss temperature is 378 °C). b) TMA curves of the GFRHybrimer film, a neat hybrimer matrix, PEN, and the glass-fabric. The CTE of the GFRHybrimer film was determined to be ~13 ppm K^{-1}. Here, for PEN, the CTE changed abruptly from 23 to 81 ppm K^{-1} at its T_g point. c) DMA curves of the GFRHybrimer film, PES, and PEN.

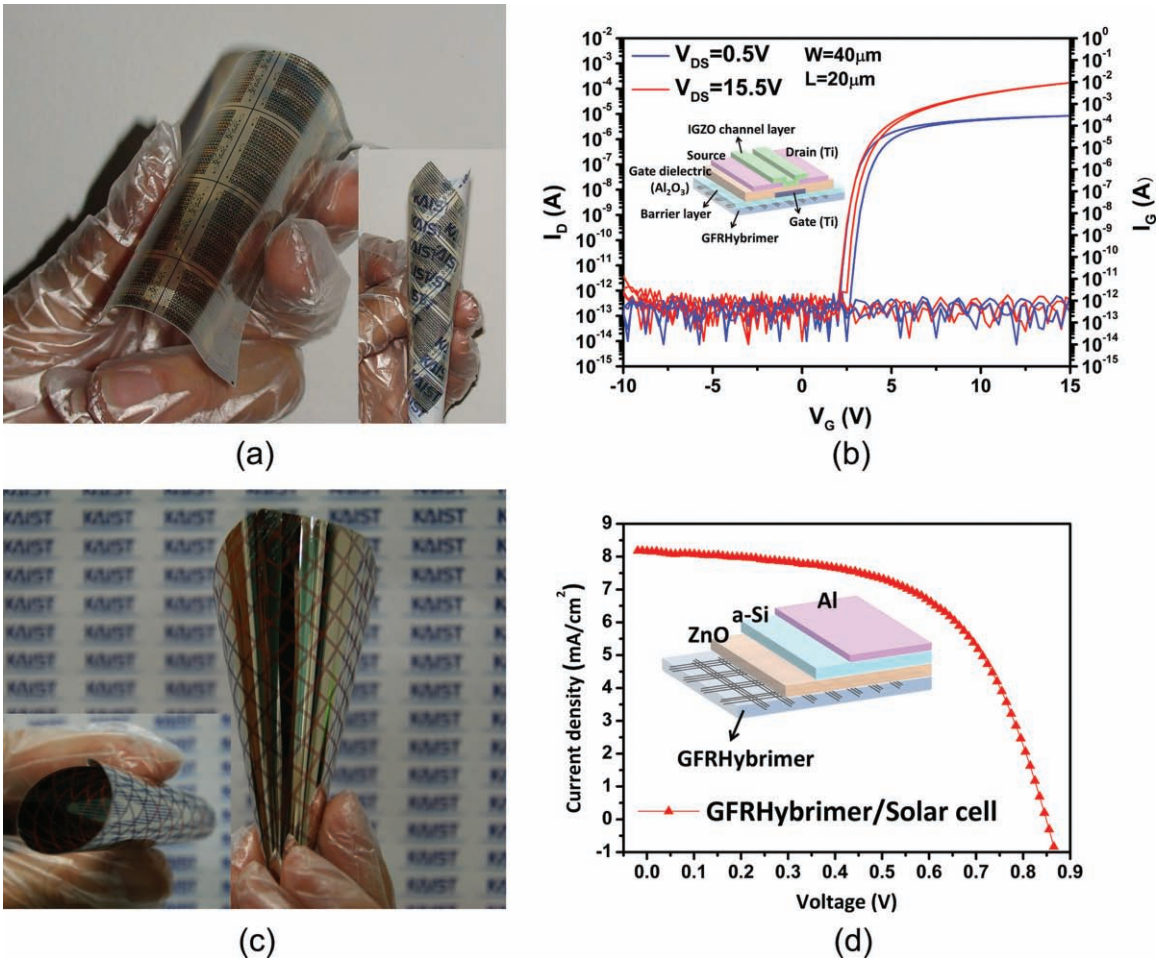

Figure 4. a) Images of flexible IGZO TFT arrays fabricated on the GFRHybrimer substrate. The IGZO TFT was fabricated at 150 °C using an ALD and a RF-sputter system. The inset image shows the rolled-up state of the IGZO TFT/GFRHybrimer backplane. b) Transfer characteristic of the IGZO TFT with a bottom gate/bottom contact structure (inset scheme). The saturation mobility was μ_{sat} = 16 cm^2 V^{-1} s^{-1} and the threshold voltage was V_{th} = 3.05 V. c) Image of a flexible a-Si based solar cell fabricated on the GFRHybrimer substrate. The solar cell was fabricated at 250 °C using a photo-CVD and a RF-PECVD system. The inset image shows the rolled-up state. d) *I–V* characteristics of the flexible solar cell. The average cell efficiency was 5.3% with a fill factor of 70%.

by fabrication of actual devices on the film. In doing so, IGZO (indium gallium zinc oxide) thin film transistor (TFT) arrays were successfully fabricated on the GFRHybrimer substrate. First, a 100 mm × 100 mm GFRHybrimer film was attached on a glass plate of the same size. The IGZO TFT was then fabricated at 150 °C using an atomic layer deposition (ALD) system and a RF-sputter system. Finally, the IGZO TFT/GFRHybrimer flexible backplane was released from the glass plate. The released IGZO/GFRHybrimer backplane was highly flexible; it could even be rolled up (**Figure 4a**). Figure 4b displays the transfer characteristics of the IGZO TFT. The electrical parameters including the saturation mobility and the threshold voltage were derived from a linear fit to the plot of the square root of I_D versus the V_G of the saturation region. The saturation mobility was μ_{sat} = 16 cm^2 V^{-1} s^{-1} and the threshold voltage was V_{th} = 3.05 V, indicating that the IGZO oxide TFT is operated in accumulation mode on a positive gate bias without any degradation of the TFT performance even after the release. The performance of GFRHybrimer substrate was tested in an even harsher environment. Arrays of a-Si based solar cells were successfully fabricated on the GFRHybrimer substrate at 250 °C with the same procedure used in the IGZO TFT fabrication. The structure of a solar cell is illustrated in Figure 4d. The aluminum electrode and transparent ZnO electrode were deposited using a RF-sputter, and the p-layer (a-SiC:H), i-layer (a-Si:H), and n-layer (a-Si:H) were deposited using a photo-assisted chemical vapor deposition (CVD) and a RF-PECVD (plasma-enhanced CVD) system. After the fabrication, the released flexible solar cell/GFRHybrimer substrate also showed sufficient flexibility to the point that it could be rolled-up (Figure 4c). *I–V* characteristics were measured, and the calculated cell efficiency was 5.3% with a fill factor of 70% (Figure 4d).

As the fabrication of high-performance electronic devices such as a-Si TFTs and oxide TFTs usually requires a high process temperature and high dimensional stability for layer integration, a flexible substrate must be equipped at least with

a low CTE and high thermal stability for the implementation of a stable flexible display. Chemical stability is another important requirement, as a flexible substrate should withstand chemically harsh environments such as that of wet-etching during a series of lithography processes. High optical transparency in a flexible substrate is also essential for typical bottom emissive displays. Unfortunately, none of the conventional plastic substrates currently available can satisfy all of these requirements. This has been a major obstacle for the straightforward implementation of a stable flexible display. We report herein a rollable high-performance transparent glass-fabric reinforced composite substrate (GFRHybrimer) with high transparency (~89%), a low CTE (~13 ppm K^{-1}) and high thermal stability (~378 °C). The performance of the GFRHybrimer substrate was tested by the fabrication of actual electronic devices using conventional glass-substrate compatible fabrication systems of ALD and CVD. The present study also provides, to the best of our knowledge, the first report of the successful fabrication of high-temperature processed devices on a novel composite-type flexible substrate.

Experimental Section

Materials: MPTMS, hydrochloric acid, and 2,2-dimethoxy-2-phenylacetophenone (BDK) were purchased from Sigma–Aldrich (St. Louis, MO). DPDMS was purchased from TCI (Tokyo, Japan). 1*H*,1*H*,2*H*, 2*H*-perfluorodecyltrimethoxysilane (PFAS) were purchased from Gelest (Morrisville, PA). Woven glass-fabrics (E-glass) ware obtained from Doosan corporation (Korea).

Preparation of Mechacryl-oligosiloxane Resin (Hybrimer Matrix): The matrix resin was synthesized by a sol–gel reaction of MPTMS and DPDMS. MPTMS and DPDMS were mixed with various Si/phenyl molar ratios (*r*) in a two-neck flask equipped with a condenser and a magnetic stirrer. HCl (0.5 N) was added to the mixture with a Si/H_2O ratio of 1.25 and refluxed at 80 °C for 1 day. After the reaction, residual solvent and H_2O were evaporated and a clear, viscous methacryl-oligosiloxane resin was obtained. The resin was then mixed with 2 wt.% of BDK as a photo-initiator.

Fabrication of GFRHybrimer Film: A glass-fabric was cut into 110 mm × 110 mm sheets and two sheets of the glass-fabric were placed on a 100 mm × 100 mm glass plate. The matrix resin was then dispensed onto the glass-fabric for impregnation. The drenched sample was then covered with another glass plate for the vacuum bag press molding process. All glass plates were surface-treated with PFAS for easy separation of the GFRHybrimer film after curing. In the vacuum bag press molding step, the sample was placed between a silicone bag and a metal plate, and sealed. When vacuum was applied, the entrapped air and excess resin in the sample were removed, providing a proper film thickness. The sample was then UV-cured using a He-lamp (365 nm) under N_2 purging, and heat-treated at 180 °C for 4 h. The GFRHybrimer film was obtained after separation from the glass plates.

Characterization of Optical/Thermo-physical Properties of the GFRHybrimer Film: For the n_D measurement, the matrix resin was cast into a 2 mm thick bulk and UV cured. *n* Ds of the bulk samples were measured by an Abbe refractometer (Bellingham and Stanley, UK). Optical transmittances of the GFRHybrimer films were measured with a UV-visible spectrophotometer (UV3101PC, Shimadzu, Japan). Thermal properties were measured by TGA (Q50, TA Instruments, Inc.) with a 5 °C min^{-1} ramp under N_2 atmosphere. Thermo-mechanical properties were measured by TMA (EXTAR TMA/SS 6100, Seiko instrument, Inc.) and DMA (2980, TA Instrument, Inc.) with a 5 °C min^{-1} ramp.

Fabrication of IGZO TFT and a-Si Solar Cell: For both the IGZO TFT and the a-Si based solar cell, the GFRHybrimer was first attached onto glass plates and devices were fabricated on the GFRHybrimer film. The IGZO TFT was fabricated at 150 °C using an ALD and a RF-sputter system. The a-Si solar cell was fabricated at 250 °C using a photo-CVD and a RF-PECVD system.

Supporting Information

Supporting information is available from the Wiley Online Library or from the author.

Acknowledgements

This research was supported by Basic Science Research Program via the National Research Foundation of Korea (NRF) funded by the Ministry of Education, Science and Technology Korea government (MEST) (CAFDC-20100009898). The authors thank Dr. Sang-Hee Ko Park (Oxide Electronics Research Team, ETRI, Korea) for technical support in IGZO TFT fabrication. The authors also thank Prof. Koeng Su Lim and Dr. Jin-Wan Jeon (Dept. Electrical Engineering, KAIST) for technical support in solar cell fabrication.

Received: June 16, 2010
Revised: July 16, 2010
Published online: September 9, 2010

[1] a) G. P. Crawford, in *Flexible Flat Panel Displays*, John Wiley & Sons Ltd., West Sussex, England **2005**; b) M.-C Choi, Y. Kim, C.-S Ha, *Prog. Polym. Sci.* **2008**, *33*, 581.

[2] a) S. H. Kim, J. H. Cheon, E. B. Kim, J. H. Bae, J. H. Hur, J. Jang, Grate, *J. Non-cryst. Solids* **2008**, *354*, 2529; b) A. Weber, S. Deutschbein, A. Plichta, A. Habeck, *SID Digest* **2002**, *6.3*, 53; c) Y.-f Chen, Y. Mei, R. Kaltofen, J. I. Monch, J. Schumann, J. Freudenberger, H.-J Klaub, O. G. Schmidt, *Adv. Mater.* **2008**, *20*, 3224.

[3] a) Z. Fan, J. C. Ho, T. Takahashi, R. Yerushalmi, K. Takei, A. C. Ford, Y.-L Chueh, A. Javey, *Adv. Mater.* **2009**, *21*, 3730; b) B. D. Gates, *Science* **2009**, *323*, 1566; c) W. A. MacDonald, *J. Mater. Chem.* **2004**, *14*, 4.

[4] a) J. Liu, B. Buchholz, R. P. H. Chang, A. Facchetti, T. J. Marks, *Adv. Mater.* **2010**, *22*, 2333; b) M.-Y Choi, D. Choi, M.-J Jin, I. Kim, S.-H Kim, J.-Y Choi, S. Y. Lee, J. M. Kim, S.-W Kim, *Adv. Mater.* **2009**, *21*, 2185; c) C. D. Sheraw, L. Zhou, J. R. Huang, D. J. Gundlach, T. N. Jackson, M. G. Kane, I. G. Hill, M. S. Hammond, J. Campi, B. K. Greening, J. Franci, J. West, *Appl. Phys. Lett.* **2002**, *80*, 1088; d) J. H. Cho, J. Lee, Y. Xia, B. Kim, Y. He, M. J. Renn, T. P. Lodge, C. D. Frisbie, *Nat. Mater.* **2008**, *7*, 900; e) J. Perelaer, M. Klokkenburg, C. E. Hendriks, U. S. Schubert, *Adv. Mater.* **2009**, *21*, 4830.

[5] a) Y. Chen, J. Au, P. Kazlas, A. Ritennour, H. Gates, M. McCreary, *Nature* **2003**, *423*, 136; b) G. H. Gelinck, H. E. Huitema, E. V. Veenendaal, E. Cantatore, L. Schrijnemakers, J. B. P. H. Van der putten, T. C. T. Geuns, M. Beenhakkers, J. B. Giesbers, B.-H Huisman, E. J. Meijer, E. M. Benito, F. J. Touwslager, A. W. Marsman, B. J. E. Van Rens, D. M. De Leeuw, *Nat. Mater.* **2004**, *3*, 106.

[6] a) Y. J. Eo, T. H. Lee, S. Y. Kim, J. K. Kang, Y. S. Han, B. S. Bae, *J. Polym. Sci., Part B: Polym. Phys* **2005**, *43*, 827; b) Y. J. Eo, J. H. Kim, J. H. Ko, B. S. Bae, *J. Mater. Res.* **2005**, *20*, 401.

[7] H. Iba, Y. Kagawa, *Philos. Mag. B* **1998**, *78*, 37.

[8] a) J. Choi, J. Harcup, A. F. Yee, Q. Zhu, R. M. Laine, *J. Am. Chem. Soc.* **2001**, *123*, 11 420; b) J. Choi, A. F. Yee, R. M. Laine, *Macromolecules* **2003**, *36*, 5666.